J Biomol NMR (2011) 51:425–435
DOI 10.1007/s10858-011-9568-3

ARTICLE

Alternative SAIL-Trp for robust aromatic signal assignment and determination of the χ_2 conformation by intra-residue NOEs

Yohei Miyanoiri · Mitsuhiro Takeda · JunGoo Jee · Akira M. Ono · Kosuke Okuma · Tsutomu Terauchi · Masatsune Kainosho

Received: 21 July 2011 / Accepted: 5 September 2011 / Published online: 23 September 2011

Abstract Tryptophan (Trp) residues are frequently found in the hydrophobic cores of proteins, and therefore, their side-chain conformations, especially the precise locations of the bulky indole rings, are critical for determining structures by NMR. However, when analyzing [U–^{13}C,^{15}N]-proteins, the observation and assignment of the ring signals are often hampered by excessive overlaps and tight spin couplings. These difficulties have been greatly alleviated by using stereo-array isotope labeled (SAIL) proteins, which are composed of isotope-labeled amino acids optimized for unambiguous side-chain NMR assignment, exclusively through the ^{13}C–^{13}C and ^{13}C–^{1}H spin coupling networks (Kainosho et al. in Nature 440:52–57, 2006). In this paper, we propose an alternative type of SAIL-Trp with the [ζ2,ζ3-^{2}H$_2$; δ1,ε3,η2-^{13}C$_3$; ε1-^{15}N]-indole ring ([^{12}C$_\gamma$,^{12}C$_{\varepsilon 2}$] SAIL-Trp), which provides a more robust way to correlate the ^{1}H$_\beta$, ^{1}H$_\alpha$, and ^{1}H$_N$ to the ^{1}H$_{\delta 1}$ and ^{1}H$_{\varepsilon 3}$ through the intra-residue NOEs. The assignment of the ^{1}H$_{\delta 1}$/^{13}C$_{\delta 1}$ and ^{1}H$_{\varepsilon 3}$/^{13}C$_{\varepsilon 3}$ signals can thus be transferred to the ^{1}H$_{\varepsilon 1}$/^{15}N$_{\varepsilon 1}$ and ^{1}H$_{\eta 2}$/^{13}C$_{\eta 2}$ signals, as with the previous type of SAIL-Trp, which has an extra ^{13}C at the C$_\gamma$ of the ring. By taking advantage of the stereospecific deuteration of one of the prochiral β-methylene protons, which was ^{1}H$_{\beta 2}$ in this experiment, one can determine the side-chain conformation of the Trp residue including the χ_2 angle, which is especially important for Trp residues, as they can adopt three preferred conformations. We demonstrated the usefulness of [^{12}C$_\gamma$,^{12}C$_{\varepsilon 2}$] SAIL-Trp for the 12 kDa DNA binding domain of mouse c-Myb protein (Myb-R2R3), which contains six Trp residues.

Keywords SAIL-Trp · Aromatic ring CH assignment · Intra-residue NOE · χ_2 conformation

Y. Miyanoiri · M. Takeda · M. Kainosho (✉)
Graduate School of Science, Structural Biology Research Center, Nagoya University, Furo-cho, Chikusa-ku, Nagoya 464-8602, Japan
e-mail: kainosho@nagoya-u.jp

J. Jee · A. M. Ono · K. Okuma · T. Terauchi · M. Kainosho
Center for Priority Areas, Tokyo Metropolitan University, 1-1 Minami-ohsawa, Hachioji 192-0397, Japan

A. M. Ono · K. Okuma · T. Terauchi
SAIL Technologies Co., Inc., 1-40 Suehiro-cho 1-chome, Tsurumi-ku, Yokohama, Kanagawa 230-0045, Japan

Introduction

The side-chain aromatic rings in proteins are important constituents of the hydrophobic core, and are also involved in various biological functions through protein–protein and protein–ligand interactions. The indole ring of the Trp residue is the largest, as compared to the other aromatic rings, and thus the side-chain conformations, i.e., χ_1 and χ_2 angles, of Trp residues significantly influence the spatial packing and dynamics of other amino acids in the surrounding hydrophobic core. However, the detailed NMR analysis of the ring signals of aromatic amino acids, using a conventional [U–^{13}C,^{15}N]-protein, has often been hampered by the extensive signal overlapping and tight spin couplings. A conventional, yet still quite useful approach to overcome this problem is to use aromatic amino acids isotopically labeled at one or more specific atom(s) in the rings (Wang et al. 1999; Jacob et al. 2002; Rajesh et al. 2003; Teilum et al. 2006). Especially, the systematic optimization of the isotope labeling pattern developed in the stereo-array isotope labeling (SAIL) method has led to extremely effective assignment schemes, as demonstrated for the aromatic ring signals of SAIL- phenylalanine (Phe)

and SAIL-tyrosine (Tyr) residues (Torizawa et al. 2005; Kainosho et al. 2006; Takeda et al. 2008, 2010). Similarly, the original SAIL-Trp (Kainosho et al. 2006), which has a [$\zeta2$,$\zeta3$-$^{2}H_2$; γ,$\delta1$,$\varepsilon2$,$\varepsilon3$,$\eta2$-$^{13}C_5$; $\varepsilon1$-^{15}N]-indole ring, can be modified to improve the observation and assignment of the ring signals. In doing so, we prepared a modified SAIL-Trp with the [$\zeta2$,$\zeta3$-$^{2}H_2$; $\delta1$,$\varepsilon3$,$\eta2$-$^{13}C_3$; $\varepsilon1$-^{15}N]-indole ring ([$^{12}C_\gamma$,$^{12}C_{\varepsilon2}$] SAIL-Trp), in which the γ and $\varepsilon2$ positions of the ring carbons were left unlabeled (Fig. 1). Since one of the prochiral β-methylene protons ($H_{\beta2}$) is stereo-selectively deuterated, as in the original SAIL-Trp, the remaining proton ($H_{\beta3}$) provides a high quality signal with unambiguous stereo-assignment (Kainosho et al. 2006; Kainosho and Güntert 2009).

In order to correlate the backbone assignment to the aromatic ring signals, a variety of scalar coupling-based experiments via $^{13}C_\gamma$ were previously developed (Yamazaki et al. 1993; Grzesiek and Bax 1995; Carlomagno et al. 1996; Prompers et al. 1997; Löhr et al. 2005). Similar pulse sequences based on the one-bond and three-bond ^{13}C–^{13}C and ^{13}C–^{1}H scalar-couplings have also been used for assigning the aromatic rings of ε- and ζ-SAIL Phe/Tyr residues (Torizawa et al. 2005). With the original SAIL-Trp, which has the [$\zeta2$,$\zeta3$-$^{2}H_2$; γ,$\delta1$,$\varepsilon2$,$\varepsilon3$,$\eta2$-$^{13}C_5$; $\varepsilon1$-^{15}N]-indole ring, this type of assignment scheme should in principle work well for assigning the $^{13}C_{\delta1}/^{1}H_{\delta1}$ and $^{15}N_{\varepsilon1}/^{1}H_{\varepsilon1}$ peaks in a SAIL-Trp residue with a γ-carbon enriched with ^{13}C. However, the intermittent ^{13}C labeling in the indole ring of SAIL-Trp does not permit the correlation of the NMR resonances of the atoms at the $\delta1/\varepsilon1$ positions to those of the $\varepsilon3/\eta2$ positions by isotropic mixing type experiments, such as HCCH-TOCSY (Fesik et al. 1990; Bax et al. 1990). Alternatively, intra-residue NOEs between the aromatic proton and aliphatic/amide protons can be used to correlate the aromatic and aliphatic protons (Billeter et al. 1982; Wüthrich 1986). The NOE-based correlation between the aliphatic side-chain and aromatic ring protons of δ-SAIL Phe/Tyr residues in a protein is a very sensitive and robust alternative assignment method (Takeda et al. 2010). In the case of Trp, since at least either one of the $^{1}H_{\delta1}$ and $^{1}H_{\varepsilon3}$ atoms is located in spatial proximity to the α, β-protons or backbone amide protons, as discussed later, a similar NOE-based assignment method for the aromatic ring signals should also work well.

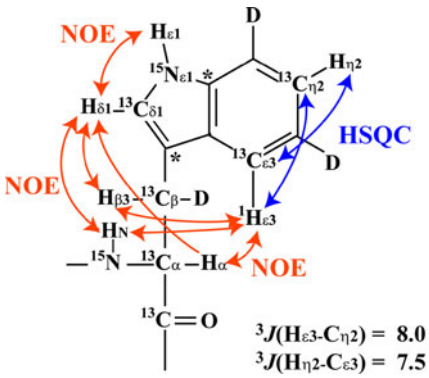

Fig. 1 Isotope labeling pattern of [$^{12}C_\gamma$,$^{12}C_{\varepsilon2}$] SAIL-Trp and the magnetization transfer pathway for the assignment. The ^{12}C atoms are not shown in the figure. In the original SAIL-Trp, the γ- and $\varepsilon2$-carbons (labeled with an *asterisk*) were ^{13}C (Kainosho et al. 2006). In this study, the γ- and $\varepsilon2$-carbons were kept as ^{12}C. The magnetization transfer pathways for assignment are depicted as *arrows*, with the names of the experiments. ^{3}J(C–H) scalar couplings were obtained as free Trp in D_2O, as described previously (van den Berg et al. 1990)

Here we present a strategy for assigning the aromatic signals of Trp residues in proteins, using a new type of SAIL-Trp, [$^{12}C_\gamma$,$^{12}C_{\varepsilon2}$] SAIL-Trp (Fig. 1). With this new SAIL-Trp, $^{1}H_{\delta1}$ and $^{1}H_{\varepsilon3}$ can be correlated by the intra-residue NOEs between the backbone/aliphatic protons (i.e., $^{1}H_{\beta3}$, $^{1}H_\alpha$ and $^{1}H_N$), as shown in Fig. 1. Another benefit of [$^{12}C_\gamma$,$^{12}C_{\varepsilon2}$] SAIL-Trp, as compared to the previous version of SAIL-Trp, which has two extra ^{13}C atoms at C_γ and $C_{\varepsilon2}$ (Kainosho et al. 2006), is that constant-time experiments are not needed to eliminate the one-bond ^{13}C–^{13}C spin couplings between C_γ and $C_{\delta1}$, leading to much higher sensitivity. Moreover, ^{1}H–^{13}C TROSY HSQC works more effectively with this new SAIL-Trp (Pervushin et al. 1997, 1998; Sørensen et al. 1997), and thus we can extend the method for much larger proteins, as compared to conventional through-bond assignment methods (Fesik et al. 1990; Bax et al. 1990).

In addition to the advantages described above, the observation of the intra-residue NOEs also provides an opportunity to determine the side-chain conformations of Trp residues. Especially, the stereo-selective mono-deuteration at the β-position in [$^{12}C_\gamma$,$^{12}C_{\varepsilon2}$] SAIL-Trp enabled us to precisely observe the NOEs between spatially proximal protons, thereby allowing the unambiguous determination of the χ_2 angle. When combined with information on the χ_1 angle, obtained by another established method (Cavanagh et al. 2006), the orientation of the indole moiety relative to the backbone can be determined. In addition, the systematic ^{13}C enrichment and deuteration allow the employment of three-bond J coupling, with a size of 7–8 Hz (Torizawa et al. 2005; Takeda et al. 2009, 2010).

We have demonstrated this assignment strategy for six Trp residues in the minimum DNA binding domain of mouse c-Myb protein (Myb-R2R3) (amino acids 89–193). The c-*myb* gene product is a transcriptional activator that plays an important role in controlling the proliferation and differentiation of hematopoietic cells (Graf 1992). Myb-R2R3 consists of two tandem repeats, R2 and R3, each containing three Trp residues (R2: Trp-95, Trp-115 and Trp-134; R3: Trp-147, Trp-166 and Trp-185). The structures of the unbound and DNA-bound forms have been determined by NMR spectroscopy (Ogata et al. 1994). The

six Trp residues constitute the hydrophobic core of each domain, and are highly conserved among homologous proteins (Ogata et al. 1994).

Materials and methods

Synthesis of SAIL-Trps

A number of syntheses concerning isotopically labeled Trp and indole have been reported (Heidelberger 1949; Bak et al. 1967; Leete and Wemple 1969; Norton and Bradbury 1976; Lautie 1979; Saito et al. 1984; van den Berg et al. 1988, 1989 and 1990; Yaw and Gawrisch 1999; Unkefer et al. 1991; Oba et al. 1995; Oba et al. 2002; Boroda et al. 2003; Osborne et al. 2003; Ilic and Cohen 2004; Soledade et al. 2006; Amir-Heidari et al. 2007; Liu et al. 2009). However, they dealt with the labeling of only a few positions in the Trp and are not suitable for ^{13}C-, ^{2}H- and ^{15}N-multi-labeling, such as in our SAIL method. We therefore, decided to develop a new general method that allows for the synthesis of any combination of ^{13}C-, ^{2}H- and ^{15}N-multi-labeling.

From the viewpoints of efficiency and economy, a wide variety of SAIL amino acids should be synthesized via common intermediates (Terauchi et al. 2008, 2011). Recently, we reported the synthesis of isotopomers of Phe and Tyr (Torizawa et al. 2005; Takeda et al. 2010). A crucial step in the reports is the hydroxybenzoate synthesis, which is flexible and accommodates the isotope labeling of any combination of ^{13}C and ^{2}H in the aromatic ring. Fortunately, the labeling pattern used for observing the $^{1}H_{\delta}$ signals of SAIL-Phe could also be used for observing the $^{1}H_{\varepsilon 3}$ and $^{1}H_{\eta 2}$ signals of the indole ring of Trp in this study. Thus, by using the labeled benzoate **1** (Scheme 1), the common intermediate of SAIL-Phe, we were able to synthesize SAIL-Trps more efficiently.

Scheme 1 shows the synthesis method of [β2,ζ2,ζ3-$^{2}H_3$; C0,α,β,δ1,ε3,η2-$^{13}C_6$; UL-$^{15}N_2$]-Trp ([$^{12}C_{\gamma}$,$^{12}C_{\varepsilon 2}$] SAIL-Trp) and [β2,ζ2,ζ3-$^{2}H_3$; C0,α,β,γ,δ1,ε2,ε3,η2-$^{13}C_8$; UL-$^{15}N_2$]-Trp (SAIL-Trp) in detail. After the conversion of hydroxyl benzoate **1** to the tetrazolyl ether derivative **2**, deoxygenation was performed using deuterium gas to give the benzoate **3**. The benzoate derivative was then converted to the benzamide **4**, which was, in turn, subjected to Hoffman rearrangement to yield the aniline **5**. Gassman indole synthesis (Gassman and Van Bergen 1974) followed by reduction (Yuan and Ajami 1982) was performed to give the indoline derivatives **8**. In this stage, the indoline derivatives were heated in D_2O, because low-intensity H_4 and H_6 signals appeared in the ^{1}H NMR spectrum by H/D exchange. The indoline **9** was then subjected to oxidation using trichloroisocyanuric acid (Tilstam et al. 2001), followed by conversion to SAIL-Trps using tryptophanase in the presence of SAIL-Ser (Vederas et al. 1978).

Computation of proton–proton distances in the Trp residue

The computations of the proton–proton distances between $H_{\beta 2}$ and $H_{\delta 1}$, $H_{\beta 2}$ and $H_{\varepsilon 3}$, $H_{\beta 3}$ and $H_{\delta 1}$, and $H_{\beta 3}$ and $H_{\varepsilon 3}$ were performed using the MATLAB software (MathWorks Inc., Natick, MA, USA), according to the procedure described by Billeter et al. (1982). The computation used the following parameters: The bond lengths are C_{α}–C_{β}: 1.53 Å; C_{β}–$H_{\beta 2/3}$: 1.08 Å; C_{β}–C_{γ}: 1.50 Å; C_{γ}–$C_{\delta 1}$: 1.37 Å; $C_{\delta 1}$–$H_{\delta 1}$: 1.08 Å; C_{γ}–$C_{\delta 3}$: 1.43 Å; $C_{\delta 3}$–$C_{\varepsilon 3}$: 1.40 Å; $C_{\varepsilon 3}$–$H_{\varepsilon 3}$: 1.08 Å. The bond angles are C_{α}–C_{β}–$H_{\beta 2/3}$: 109.0°; C_{α}–C_{β}–C_{γ}: 113.3°; C_{β}–C_{γ}–$C_{\delta 1}$: 126.8°; C_{γ}–$C_{\delta 1}$–$H_{\delta 1}$: 124.3°; C_{β}–C_{γ}–$C_{\delta 3}$: 126.9°; C_{γ}-$C_{\delta 3}$-$C_{\varepsilon 3}$: 133.8°; $C_{\delta 3}$-$C_{\varepsilon 3}$-$H_{\varepsilon 3}$: 121.3°.

Statistics for torsion angles and distances of Trp

To take the sequence redundancy and inaccuracy in local geometries into account, we chose the structures in the Top 500 database (http://kinemage.biochem.duke.edu/databases/top500.php), in which all of the structures have a resolution better than 1.8 Å. We retrieved data from a total of 1,553 Trp residues. The pairs of torsion angles, χ_1 and χ_2, of these Trp residues were classified by the *K*-means algorithm of the MATLAB software (Press et al. 1986) into seven relatively well populated conformational clusters, with the means and standard deviations of the various inter-atom distances for each cluster, as shown in Table 1.

Expression and purification of Myb-R2R3 selectively labeled with [$^{12}C_{\gamma}$,$^{12}C_{\varepsilon 2}$] SAIL-Trp residues

The DNA encoding mouse Myb-R2R3 (amino acids 89–193) was amplified by PCR, and cloned into the pET3a vector (Novagen). The resulting plasmid, pMybR2R3, was then transformed into *E. coli* Rosetta (DE3) pLysS competent cells (Novagen). The cells were grown at 37°C in M9 minimal medium, containing $^{15}NH_4Cl$ as the sole nitrogen source. When the A_{600} value reached about 0.5, 5 mg of [$^{12}C_{\gamma}$,$^{12}C_{\varepsilon 2}$] SAIL-Trp was added to 1 l of the culture medium. After 1 h, isopropyl-β-D-1-thiogalactopyranoside (IPTG) was added to a final concentration of 1 mM, and the induction was conducted for 6 h.

The Myb-R2R3 protein was purified by the method described previously (Ogata et al. 1994), with a slight modification. Briefly, the lysate was centrifuged at 20,000×*g* for 30 min at 4°C. Ammonium sulfate was then added to the supernatant to 50%. After centrifugation at 20,000×*g* for 30 min, ammonium sulfate was added to the supernatant to 80%. After centrifugation at 20,000×*g* for

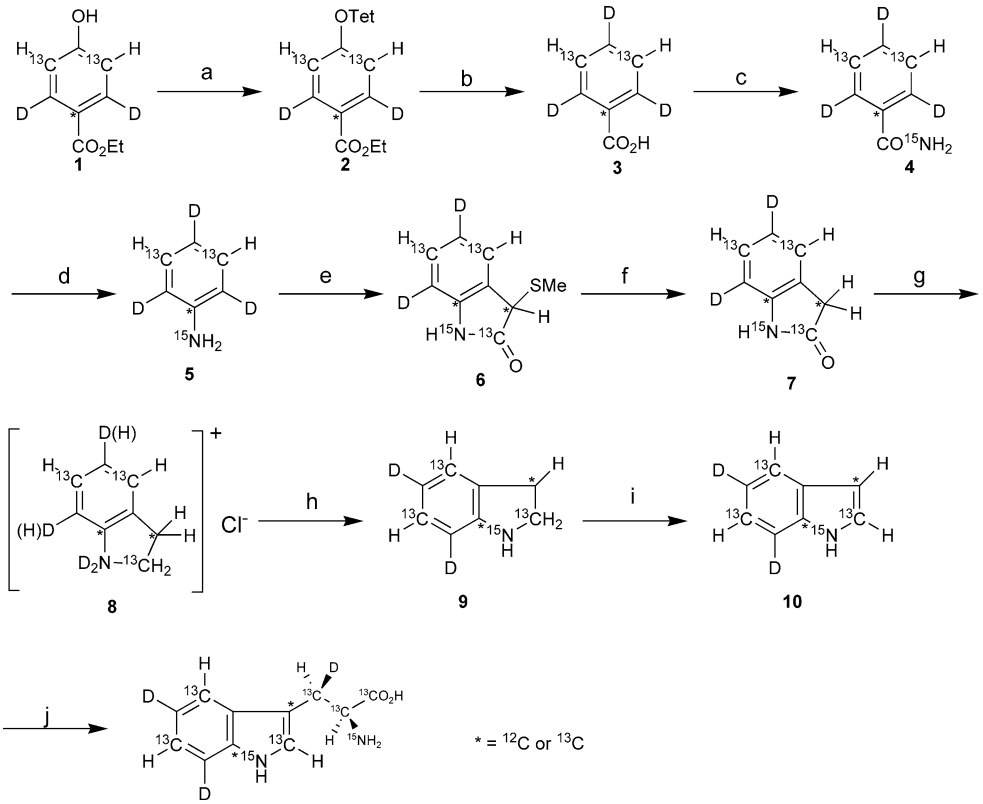

Scheme 1 Preparation of [β2,ζ2,ζ3-$^{2}H_3$; C0,α,β,δ1,ε3,η2-$^{13}C_6$; UL-$^{15}N_2$]- and [β2,ζ2,ζ3-$^{2}H_3$; C0,α,β,γ,δ1,ε2,ε3,η2-$^{13}C_8$; UL-$^{15}N_2$]-Trp. Reagents and Conditions: *a* 5-chloro-1-phenyl-1H-tetrazole, K_2CO_3, acetone; *b* **1** Pd/C, Na_2CO_3, D_2, benzene, **2** NaOH, MeOH; *c* **1** $SOCl_2$, **2** $CH_3CO_2^{15}NH_4$, acetone; *d* NaOCl, Δ; *e* MeS*$CH_2^{13}CO_2Et$, *tert*-BuOCl, Et_3N; *f* Raney-Ni/EtOH; (g) **1** $LiBH_4$, BF_3Et_2O, **2** DCl; *h* D_2O, Δ; *i* trichloroisocyanuric acid, DBU; *j* SAIL-Ser, Tryptophanase

30 min, the precipitate was suspended and dialyzed against 20 mM potassium phosphate buffer (pH 6.8) containing 10 mM dithiothreitol (DTT). The dialyzed sample was loaded onto a cation exchange column, and was eluted with a NaCl concentration gradient from 0 to 1 M. The eluted protein samples were applied to a gel filtration column. Finally, the protein was dialyzed against 100 mM potassium phosphate buffer (pH 6.8), containing 20 mM DTT and 1 mM sodium azide (NaN_3). Approximately 2 mg of purified [$^{12}C_{\gamma}$,$^{12}C_{\varepsilon 2}$] SAIL-Trp labeled Myb-R2R3 protein were obtained per 1 l of the M9 culture medium containing 5 mg [$^{12}C_{\gamma}$,$^{12}C_{\varepsilon 2}$] SAIL-Trp, in which more than 90% of the Trp residues were labeled with [$^{12}C_{\gamma}$,$^{12}C_{\varepsilon 2}$] SAIL-Trp, according to the mass spectrometric analysis (data not shown).

Synthesis and purification of the target DNA oligomers

A 16-base DNA oligomer, d(CCTAACTGACACACAT), and its complementary strand, synthesized with a DNA synthesizer and purified by HPLC, were purchased from SIGMA. They were annealed and further purified, as described previously (Ogata et al. 1994).

NMR spectroscopy

The Myb-R2R3 protein, residue-selectively labeled with [$^{12}C_{\gamma}$,$^{12}C_{\varepsilon 2}$] SAIL-Trp, was concentrated to 0.5 mM in a volume of 280 µl. The NMR sample buffer contained 100 mM potassium phosphate (pH 6.8), 20 mM DTT, 1 mM NaN_3 and either 90% H_2O/10% D_2O or 100% D_2O. Unless stated otherwise, NMR measurements were performed on a DRX800 spectrometer (Bruker Biospin; 800.39 MHz for ^{1}H) equipped with a TXI triple resonance cryogenic probe at 17°C.

The [$^{12}C_{\gamma}$,$^{12}C_{\varepsilon 2}$] SAIL-Trp-labeled Myb-R2R3: DNA complex was prepared as described previously (Ogata et al. 1994). The complex sample was concentrated to 0.5 mM in salt-free solutions (pH 6.8), containing 20 mM DTT, 1 mM NaN_3 and either 90% H_2O/10% D_2O or 100% D_2O. The protein/DNA molar ratio was 1:1.5. The NMR measurements for the complex sample were performed at 37°C.

The NMR spectra were measured using the samples in 90% H_2O/10% D_2O, except for the ^{1}H–^{13}C HSQC spectra (Bodenhausen and Ruben 1980), which were obtained using the 100% D_2O sample. In the 2D ^{1}H–^{13}C HSQC and that with the TROSY method on t_1 correlation experiments (Pervushin et al. 1997, 1998; Sørensen et al. 1997), the data size and the spectral width were 256 (t_1) × 1024 (t_2) and 3,200 Hz (ω_1, ^{13}C) × 11,200 Hz (ω_2, ^{1}H), respectively. The carrier frequencies of ^{1}H and ^{13}C were 4.7 and 122 ppm, respectively. The number of scans/FID was 64, and the repetition time was 1.1 s. In the 2D ^{1}H–^{13}C HSQC experiments for correlating the ε3 and η2 positions, the data size and the spectral width were 128 (t_1) × 1024 (t_2)

Table 1 Possible conformational clusters of the Trp side-chain residues and patterns of observable intra-residue NOEs

No.	%	Torsion angles (°)		Distances between two atoms (Å)							
		$\chi1$	$\chi2$	Hβ2-Hδ1	Hβ3-Hδ1	HN-Hδ1	Hα-Hδ1	Hβ2-Hε3	Hβ3-Hε3	HN-Hε3	Hα-Hε3
1	31.3	−67.1	98.7	**2.67**	3.78	**3.03**	4.28	4.14	**2.71**	5.12	**2.88**
		(12.0)	(17.2)	(0.12)	(0.12)	(0.39)	(0.28)	(0.12)	(0.21)	(0.42)	(0.48)
2	17.6	−167.5	74.7	**2.79**	3.88	4.93	**3.05**	4.04	**2.54**	4.70	4.59
		(18.9)	(20.7)	(0.17)	(0.05)	(0.23)	(0.32)	(0.18)	(0.12)	(0.19)	(0.29)
3	16.6	−167.2	−104.7	3.58	**2.64**	5.05	4.35	**2.76**	4.18	4.55	**2.74**
		(19.4)	(15.1)	(0.11)	(0.09)	(0.15)	(0.23)	(0.20)	(0.08)	(0.33)	(0.42)
4	11.8	−68.4	−5.25	3.72	3.60	3.23	**2.37**	**2.81**	**3.01**	4.87	5.13
		(9.4)	(21.57)	(0.15)	(0.18)	(0.47)	(0.22)	(0.26)	(0.30)	(0.44)	(0.14)
5	9.0	61.5	−89.8	3.85	**2.72**	**2.77**	4.45	**2.58**	4.11	4.98	4.30
		(11.0)	(10.7)	(0.06)	(0.10)	(0.49)	(0.12)	(0.12)	(0.10)	(0.36)	(0.17)
6	5.3	60.4	88.4	**2.72**	3.85	4.42	4.46	4.10	**2.58**	3.18	4.27
		(10.1)	(12.9)	(0.11)	(0.06)	(0.39)	(0.13)	(0.11)	(0.12)	(0.57)	(0.17)
7	4.7	−68.8	−88.2	3.86	**2.74**	5.01	3.13	**2.57**	4.08	**2.73**	4.50
		(14.1)	(16.1)	(0.06)	(0.14)	(0.42)	(0.31)	(0.13)	(0.15)	(0.56)	(0.31)

Values in parentheses are SD. Distances shorter than 3.1 Å are written in bold. While Hβ2 is deuterated in [$^{12}C_{\gamma}$,$^{12}C_{\varepsilon2}$] SAIL-Trp, the corresponding distance is provided, for reference

and 8,100 Hz (ω_1, ^{13}C) × 11,700 Hz (ω_2, ^{1}H), respectively. In the INEPT, which is composed of [$(\pi/2)_x$(^{1}H)-τ-π (^{1}H,^{13}C)-τ-$(\pi/2)_y$(^{1}H)], the delay τ was 6.1 ms when correlating $^{1}H_{\varepsilon3}$–$^{13}C_{\eta2}$ or $^{1}H_{\eta2}$–$^{13}C_{\varepsilon3}$ via three-bond scalar coupling. Although this delay time was much shorter than the calculated optimal value of ca. 31 ms for the $^{3}J_{CH}$ between $^{1}H_{\varepsilon3}$ and $^{13}C_{\eta2}$ or $^{1}H_{\eta2}$–$^{13}C_{\varepsilon3}$, which are both about 8 Hz, we found 6.1 ms to be a good compromise between the optimal delay and fast relaxation times. The carrier frequencies of protons and carbons were 4.7 and 125.5 ppm, respectively, and the number of scans/FID was 256. The repetition time was 2 s.

The 3D ^{13}C-edited NOESY-HSQC experiment (Kay et al. 1989) was performed with a mixing time of 100 ms. The data size and the spectral width were 128 (t_1) × 20 (t_2) × 2,048 (t_3) points and 11,100 Hz (ω_1, ^{1}H) × 2,400 Hz (ω_2, ^{13}C) × 11,100 Hz (ω_3, ^{1}H), respectively. The number of scans/FID was 48, and the repetition time was 1.2 s. The carrier frequencies of ^{1}H and ^{13}C were 4.7 and 122 ppm, respectively.

The NMR chemical shift perturbation of Myb-R2R3 labeled by [$^{12}C_{\gamma}$,$^{12}C_{\varepsilon2}$] SAIL-Trp, upon binding to the target DNA, was performed on a DRX800 spectrometer equipped with a TXI cryogenic probe at 37°C. The ^{1}H–^{13}C correlation experiments for the unbound and DNA-bound forms were both acquired using ^{1}H–^{13}C TROSY HSQC. The data size and spectral width were 256 (t_1) × 2,048 (t_2) and 3,200 Hz (ω_1, ^{13}C) × 11,200 Hz (ω_2, ^{1}H), respectively. The number of scans/FID was 256, and the repetition time was 1.2 s. The carrier frequencies of ^{1}H and ^{13}C were 4.7 and 121 ppm, respectively.

Results and discussion

The assignment of $^{1}H_{\delta1}$ and $^{1}H_{\varepsilon3}$ peaks by NOE with $^{1}H_{\beta3}$, $^{1}H_{\alpha}$ and $^{1}H_{N}$ protons

The assignment of the aromatic peaks in [$^{12}C_{\gamma}$,$^{12}C_{\varepsilon2}$] SAIL-Trp began by correlating the $^{13}C_{\delta1}$/$^{1}H_{\delta1}$ and $^{13}C_{\varepsilon3}$/$^{1}H_{\varepsilon3}$ peaks to the backbone/aliphatic peaks (i.e., $^{1}H_{\beta3}$, $^{1}H_{\alpha}$ and $^{1}H_{N}$ peaks) previously assigned by the intra-residue NOEs (Fig. 1).

In the case of Phe and Tyr residues, the χ_2 angles have a preference for two regions: ∼+90° and ∼−90° (Ponder and Richards 1987; Schrauber et al. 1993; Dunbrack and Karplus 1993). On the other hand, the χ_2 angles of Trp had preferences for three different regions: ∼+90°, ∼0° and ∼−90° (Dunbrack and Cohen 1997). In accordance with this, our survey of the Trp side-chain conformations, using the TOP500 structure database, revealed that there are three favorable conformational clusters with respect to the χ_2 angle. In addition, when the χ_2 angles are ∼+90° and ∼−90°, there are three clusters with respect to the χ_1 angle (i.e., ∼+60°, ∼180° and ∼−60°). On the other hand, when the χ_2 angle is ∼0°, only the χ_1 angle of ∼−60° is highly populated (Fig. 2).

In addition, the two preferred angles of ∼+90° and ∼−90° in Phe and Tyr residues are practically identical, due to the symmetry of the aromatic rings. However, the Trp residue is unsymmetrical with respect to the 180° rotation about the C_{β}–C_{γ} axis, and thus the spatial proximity of the proton pairs of interest is largely affected by

the rotameric conformation in the case of Trp, as compared with those of Phe and Tyr.

It is therefore, important to understand the relationship between the spatial proximity of each proton pair and the rotameric conformation of the Trp residue. Here, we focused on the seven preferred rotameric conformations, which correspond to 96.3% of the total conformations, and surveyed the proton–proton distance of interest for each conformation (Table 1). In most conformations, at least one of the $^{1}H_{\beta3}$, $^{1}H_{\alpha}$ and $^{1}H_{N}$ atoms is located within 3.1 Å of the $^{1}H_{\delta1}$ atom, which is also the case for the $^{1}H_{\varepsilon3}$ atom. (Here $^{1}H_{\beta2}$ is not considered, because it is deuterated.) Therefore, the $^{1}H_{\delta1}$ and $^{1}H_{\varepsilon3}$ peaks can, in most cases, be correlated with either of the previously assigned backbone/aliphatic protons by intra-residue NOEs. For example, in the most preferred conformation ($\chi_1 = -67 \pm 12°$, $\chi_2 = -99 \pm 17°$), the $^{1}H_{\delta1}$ and $^{1}H_{\varepsilon3}$ protons are spatially proximal to the $^{1}H_{N}$ and $^{1}H_{\beta3}$ protons, respectively, which ensures the observation of NOEs between $^{1}H_{\delta1}$ and $^{1}H_{N}$ and between $^{1}H_{\varepsilon3}$ and $^{1}H_{\beta3}$.

To demonstrate this, we observed the intra-residue NOEs using the 12 kDa DNA binding domain of Myb (Myb-R2R3), selectively labeled with [$^{12}C_{\gamma}$,$^{12}C_{\varepsilon2}$] SAIL-Trp. In this case, we used [$^{12}C_{\gamma}$,$^{12}C_{\varepsilon2}$] SAIL-Trp, rather than original SAIL-Trp, to eliminate the $^{13}C_{\delta1}$–$^{13}C_{\gamma}$ spin coupling (70–75 Hz) and observe $^{1}H_{\delta1}$/$^{13}C_{\delta1}$ peaks with high intensity and resolution (Fig. 1). As shown in Fig. 3, for all of the $^{1}H_{\delta1}$ and $^{1}H_{\varepsilon3}$ protons of Trp, intra-residue NOEs with either the $^{1}H_{\alpha}$, $^{1}H_{\beta3}$ or $^{1}H_{N}$ proton were observed, which led to the assignment of the $^{1}H_{\delta1}$ and $^{1}H_{\varepsilon3}$ peaks.

In addition, the observed intra-residue NOEs, especially between $^{1}H_{\delta1}$ and $^{1}H_{\beta3}$ or $^{1}H_{\varepsilon3}$ and $^{1}H_{\beta3}$, provide information on the χ_2 angle. As shown in Fig. 4, when the χ_2 angle is $\sim+90°$, a strong NOE is observed between $^{1}H_{\varepsilon3}$ and $^{1}H_{\beta3}$. When the χ_2 angle is $\sim-90°$, a strong NOE between $^{1}H_{\delta1}$ and $^{1}H_{\beta3}$ is observed. When χ_2 is around $\sim0°$, a weak NOE between $^{1}H_{\varepsilon3}$ and $^{1}H_{\beta3}$ and a strong NOE between $^{1}H_{\delta1}$ and $^{1}H_{\alpha}$ are observed. In the case of Myb-R2R3, the first case corresponds to Trp-95, Trp-115, Trp-147 and Trp-166, the second case corresponds to Trp-134 and Trp-185, and the last case is not included, which is in agreement with the χ_2 value of Trp in the crystal structure (Fig. 3).

If ambiguity remains, then an additional experiment using another type of [$^{12}C_{\gamma}$,$^{12}C_{\varepsilon2}$] SAIL-Trp, in which $^{1}H_{\beta3}$ is mono-deuterated and $^{1}H_{\beta2}$ keeps ^{1}H, would be useful. As shown in Table 1 and Fig. 4, the NOEs observed for the $^{1}H_{\beta2}$–$^{1}H_{\delta1}$/$^{1}H_{\beta2}$–$^{1}H_{\varepsilon3}$ pairs are complementary to those for the $^{1}H_{\beta3}$–$^{1}H_{\delta1}$/$^{1}H_{\beta3}$–$^{1}H_{\varepsilon3}$ pairs. By combining the results of the two [$^{12}C_{\gamma}$,$^{12}C_{\varepsilon2}$] SAIL-Trps with different stereo-selectivities of mono-deuteration, the χ_2 angle can be determined unambiguously.

It should be noted that, in the case of proteins labeled with [U–^{13}C/^{15}N] Trp, an attempt to relate the intra-residue NOEs between the aromatic and β-protons would not prove fruitful, since the spin diffusion of the NOE via $^{1}H_{\beta2}$ generates NOEs between spatially distal protons. In addition, the stereo-specific assignment of the two methylene protons in [U–^{13}C/^{15}N] Trp is frequently troublesome. The use of [$^{12}C_{\gamma}$,$^{12}C_{\varepsilon2}$] SAIL-Trp circumvents the laborious stereo-specific assignment step.

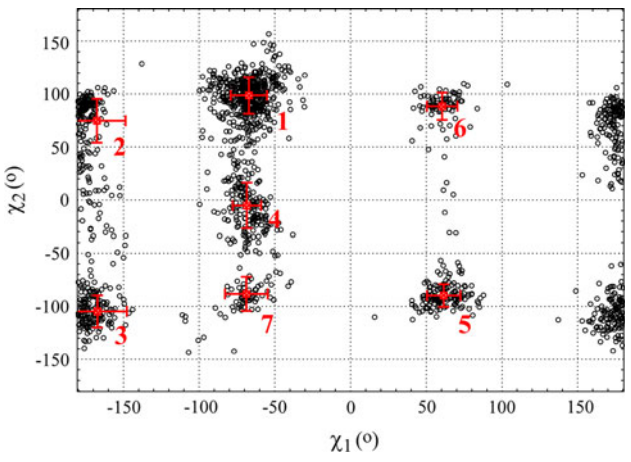

Fig. 2 Distribution of side-chain χ_1 and χ_2 dihedral angles in Trp residues in proteins. These data are derived from the TOP500 structure database (http://kinemage.biochem.duke.edu/databases/top500.php). The *red* zone is the major conformation. The clusters are labeled with *numbers*, in the order of their population

Assignment of the $\varepsilon1/\eta2$ resonance in the [$^{12}C_{\gamma}$,$^{12}C_{\varepsilon2}$] SAIL-Trp residue

Once the $^{1}H_{\delta1}$ and $^{1}H_{\varepsilon3}$ peaks have been assigned, the next step is the assignment of $^{1}H_{\varepsilon1}$/$^{15}N_{\varepsilon1}$ and $^{1}H_{\eta2}$/$^{13}C_{\eta2}$. The $^{1}H_{\varepsilon1}$ could readily be correlated to $^{1}H_{\delta1}$ by the vicinal NOE, without any difficulty (Figs. 1, 3). The assignment of the $^{1}H_{\eta2}$/$^{13}C_{\eta2}$ resonances was performed by correlating the $^{1}H_{\varepsilon3}$/$^{13}C_{\varepsilon3}$ resonances to $^{1}H_{\eta2}$/$^{13}C_{\eta2}$ via the $^{1}H_{\varepsilon3}$–$^{13}C_{\eta2}$ or $^{1}H_{\eta2}$–$^{13}C_{\varepsilon3}$ three-bond scalar coupling ($\sim$8 Hz). While the magnetization transfer though such a long range coupling does not work in the case of [U–^{13}C/^{15}N] Trp, the atom-specific ^{2}H- and ^{13}C-labeling in [$^{12}C_{\gamma}$,$^{12}C_{\varepsilon2}$] SAIL-Trp permits efficient magnetization transfer (Torizawa et al. 2005; Takeda et al. 2009, 2010). In this magnetization transfer process, we employed an HSQC pulse scheme, and in INEPT, composed of [$(\pi/2)_x$(^{1}H)-τ-π (^{1}H,^{13}C)-τ-$(\pi/2)_y$(^{1}H)], the delay τ was adjusted to multiples of $1/(2^{1}J_{CH})$, such that the evolution due to $^{1}J_{CH}$ ($^{1}H_{\varepsilon3}$–$^{13}C_{\varepsilon3}$ and $^{1}H_{\eta2}$–$^{13}C_{\eta2}$) was refocused. Through the observation of the $^{1}H_{\varepsilon3}$–$^{13}C_{\eta2}$ and $^{1}H_{\eta2}$–$^{13}C_{\varepsilon3}$ correlation peaks, the $^{13}C_{\eta2}$/$^{1}H_{\eta2}$ peaks of Myb-R2R3 were unambiguous assigned (Fig. 5). Presumably, conventional hetero-nuclear multi-bond correlation spectroscopy (HMBC) (Bax and Summers 1986) should also work in this case.

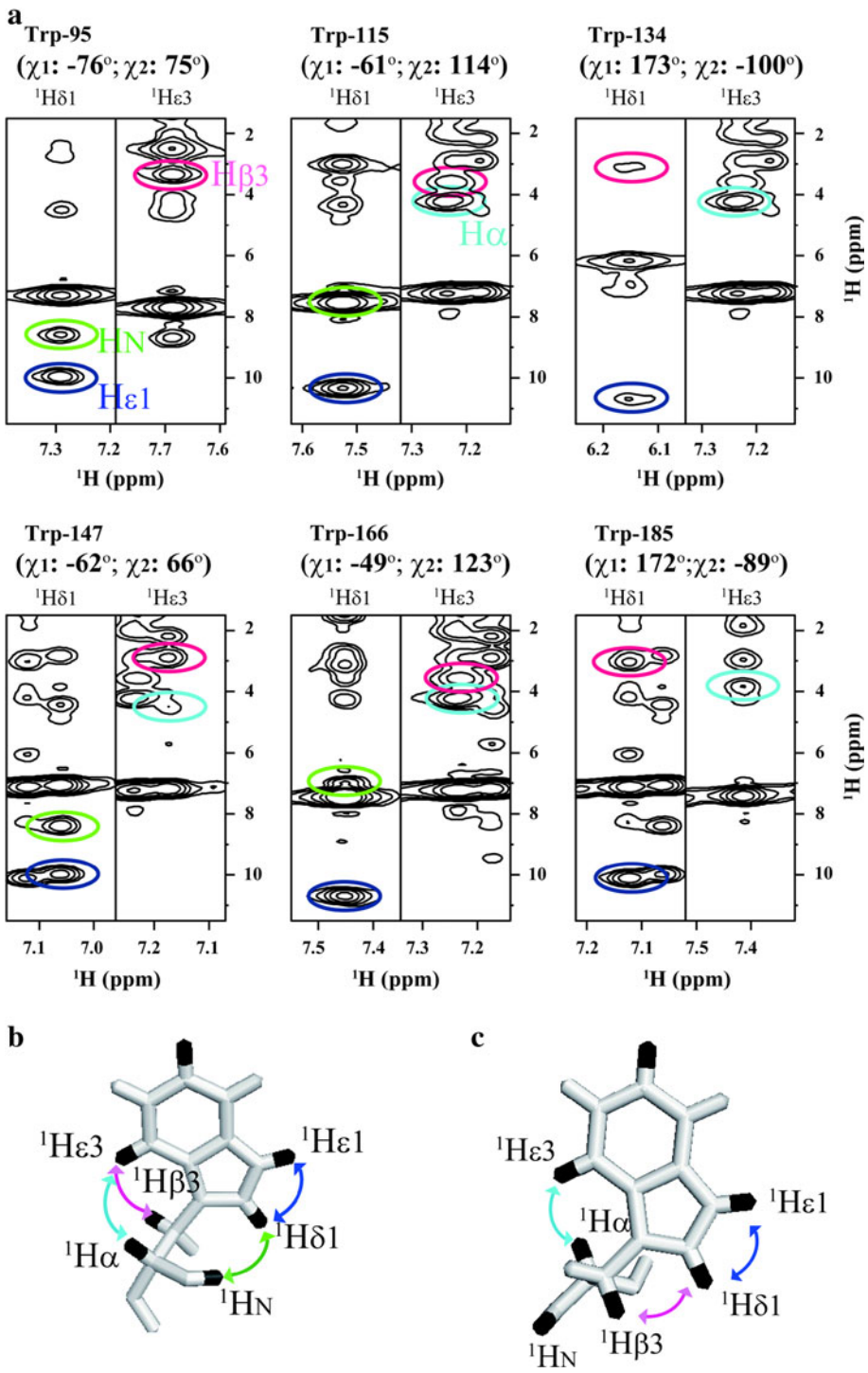

Fig. 3 Intra-residue NOEs between the aromatic and aliphatic/amide protons with patterns dependent on the side-chain conformation. **a** ^{1}H–^{1}H strips from the 3D ^{1}H–^{13}C NOESY-HSQC spectrum of Myb-R2R3 residue-selectively labeled by [$^{12}C_{\gamma}$,$^{12}C_{\varepsilon 2}$] SAIL-Trp (0.5 mM sample concentration), taken at the $^{13}C_{\delta 1}$ and $^{13}C_{\varepsilon 3}$ chemical shifts of the six Trp residues. Intra-residue NOEs with $^{1}H_{N}$, $^{1}H_{\alpha}$, $^{1}H_{\beta 3}$ and $^{1}H_{\varepsilon 1}$ are marked by *green*, *cyan*, *red* and *blue circles*, respectively. Above the spectra, the values of the χ_1 and χ_2 angles in the corresponding crystal structure (PDB# 1GV2) are described. The ϕ angles of the Trp residues are Trp-95: −86°; Trp-115: −54°; Trp-134: −70°; Trp-147: −122°; Trp-166: −54°; Trp-185: −66°. The NOESY data were acquired on a DRX800 spectrometer at 17°C. The NOE mixing time was 100 ms. As representative cases of χ_2 of ∼+90° and ∼−90°, the rotameric conformations are displayed for Trp-147 (**b**) and Trp-185 (**c**), respectively. In **b** and **c**, the observed intra-residue NOEs are displayed as *arrows*, with colors corresponding to those in (**a**)

The NMR spectra of Myb-R2R3 selectively labeled with [$^{12}C_{\gamma}$,$^{12}C_{\varepsilon 2}$] SAIL-Trp

Through the aforementioned assignment procedures, the three ^{1}H–^{13}C aromatic peaks of each [$^{12}C_{\gamma}$,$^{12}C_{\varepsilon 2}$] SAIL-Trp residue within the Myb-R2R3 protein were exclusively assigned. As compared to the spectrum of Myb-R2R3 labeled with UL-Trp (data not shown), the spectrum of Myb-R2R3 labeled with [$^{12}C_{\gamma}$,$^{12}C_{\varepsilon 2}$] SAIL-Trp was improved, by virtue of the elimination of the one-bond ^{13}C–^{13}C coupling and the deleterious ^{1}H–^{1}H dipole interactions (Fig. 6). Finally, we successfully completed the assignment of the Trp residues of Myb-R2R3 using SAIL-Trp, a feat that could not have been accomplished using a conventional, uniformly ^{13}C,^{15}N-double labeled sample (Ogata et al. 1994). In the case of Myb-R2R3, the signal of

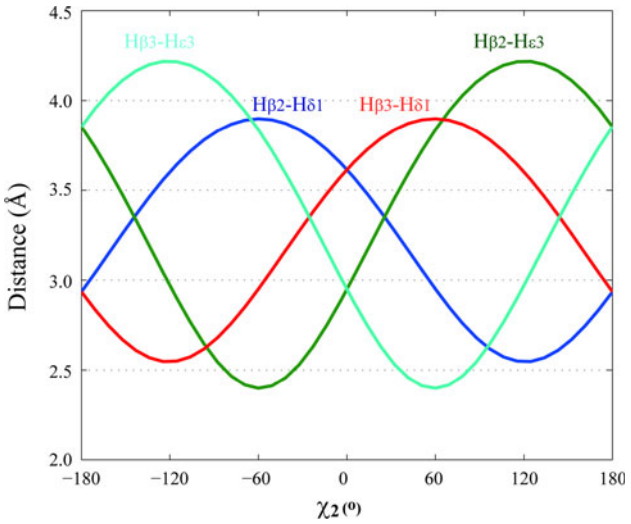

Fig. 4 The dependence of the distance between the backbone/aliphatic and aromatic protons on the rotameric conformation of the Trp residue. The proton–proton distances were simulated for pairs of $H_{\beta 2}$–$H_{\delta 1}$, $H_{\beta 2}$–$H_{\varepsilon 3}$, $H_{\beta 3}$–$H_{\delta 1}$ and $H_{\beta 3}$–$H_{\varepsilon 3}$. This computation was performed with fixed bond lengths and bond angles, using the Matlab software (Mathworks Inc.), according to a previously described procedure (Billeter et al. 1982). The values of the parameters are described in the "Materials and methods"

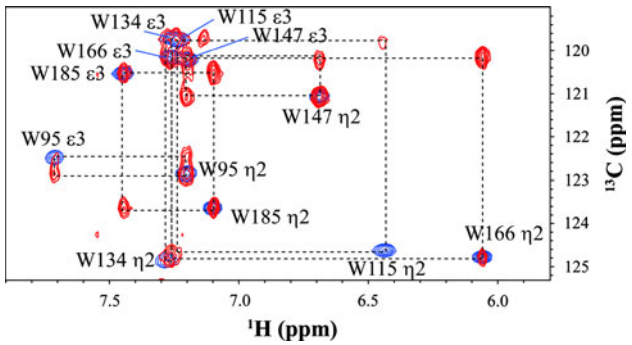

Fig. 5 Assignment of the $^{13}C_{\eta 2}/^{1}H_{\eta 2}$ peaks by three bond *J* coupling with $^{13}C_{\varepsilon 3}/^{1}H_{\varepsilon 3}$. ^{1}H–^{13}C HSQC spectra of Myb-R2R3 selectively labeled by [$^{12}C_{\gamma}$,$^{12}C_{\varepsilon 2}$] SAIL-Trp, acquired at different INEPT time delays. In the INEPT spectra, composed of $[(\pi/2)_x(^{1}H)$-τ-π $(^{1}H,^{13}C)$-τ-$(\pi/2)_y(^{1}H)]$, the delay τ values were 1.5 ms (*blue*) and 6.1 ms (*red*). In the spectra, $^{1}H_{\varepsilon 3}/^{13}C_{\varepsilon 3}$ and $^{1}H_{\eta 2}/^{13}C_{\eta 2}$ peaks are labeled with their assignments

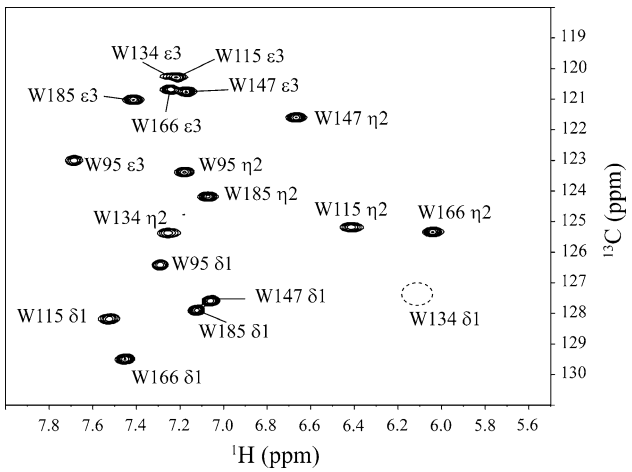

Fig. 6 NMR spectra of Myb-R2R3 selectively labeled with [$^{12}C_{\gamma}$,$^{12}C_{\varepsilon 2}$] SAIL-Trp. ^{1}H–^{13}C TROSY-HSQC spectrum of 0.5 mM of Myb-R2R3 residue-selectively labeled by [$^{12}C_{\gamma}$,$^{12}C_{\varepsilon 2}$] SAIL-Trp. The peaks are labeled with their assignments. The data were acquired on a DRX800 spectrometer at 17°C. The peak intensity of the $^{1}H_{\delta 1}/^{13}C_{\delta 1}$ signal of Trp-134, marked by a *dashed circle*, was weaker than those of other peaks, probably due to exchange broadening

Trp-134 $^{1}H_{\delta 1}/^{13}C_{\delta 1}$ was weaker relative to the other peaks, probably due the exchange-broadening arising from the previously reported instability of the third helix in R2 (Myrset et al. 1993).

The feasibility of assigning the aromatic peaks in [$^{12}C_{\gamma}$,$^{12}C_{\varepsilon 2}$] SAIL-Trp residues generates an opportunity to proceed to further NMR studies, including the structures, dynamics and interactions of proteins. As a case study of an interaction analysis, we performed chemical shift perturbation experiments for the assigned Trp aromatic peaks by adding the target 16-base-pair DNA oligomer [d(CCTA-ACTGACACACAT)]$_2$. As shown in Fig. 7a, many of the signals underwent chemical shift changes upon binding to the target DNA. As the dissociation constant between the Myb-R2R3 and the DNA is on the order of 10^{-9} M (Tanikawa et al. 1993), the binding was within the slow exchange regime on the NMR time scale, and the aromatic peaks of the DNA-bound form were analyzed in the same way, independently of the free form (data not shown). Intriguingly, relatively large chemical shift changes were observed for the Trp residues distal from the binding site (e.g., Trp-95 and Trp-147), rather than those located within the binding site (e.g., Trp-115 and 166) in the complex structure (PDB code: 1MSE) (Fig. 7b, c). Considering that the largely perturbed Trp indole ring constitutes the hydrophobic core in the tandem repeat, the chemical shift is assumed to be caused by the subtle rearrangement of helices upon binding to the target DNA, implying the potential of the aromatic peaks of Trp residues to serve as probes to detect such subtle conformational rearrangements occurring in the structural core.

Conclusions

In this study, we present a strategy for assigning the aromatic resonances ($\delta 1$, $\varepsilon 1$, $\varepsilon 3$ and $\eta 2$ peaks) of [$^{12}C_{\gamma}$,$^{12}C_{\varepsilon 2}$] SAIL-Trp residues, which has provided new insights into the mechanism of Myb-R2R3 binding to its target DNA.

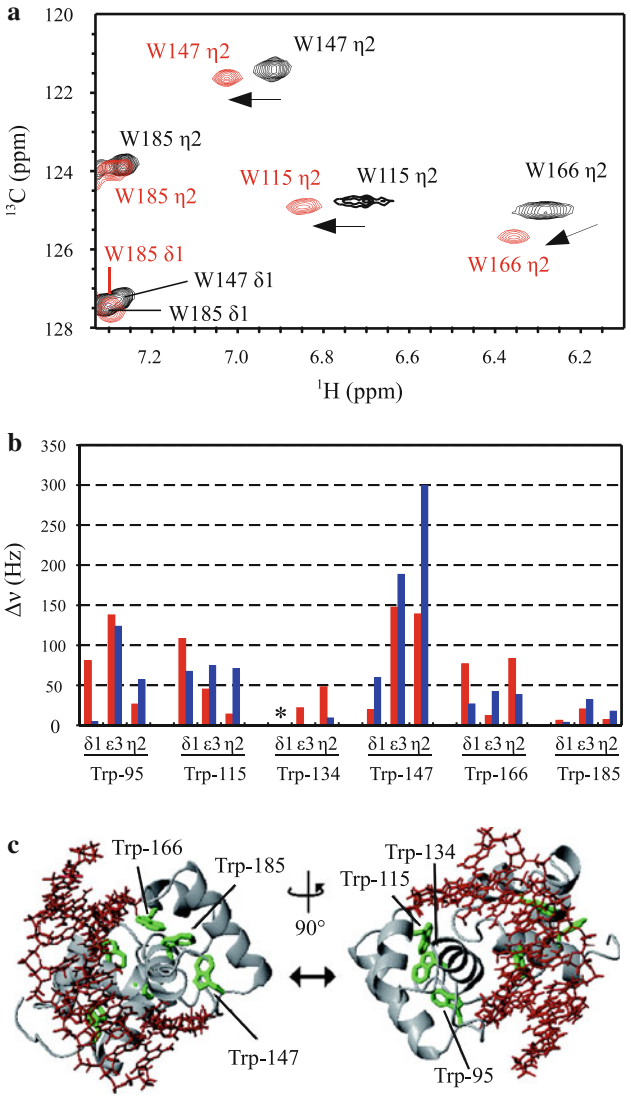

Fig. 7 Chemical shift perturbation experiments for aromatic peaks of [$^{12}C_{\gamma}$,$^{12}C_{\varepsilon 2}$] SAIL-Trp residues in Myb-R2R3. **a** Overlay of ^{1}H–^{13}C TROSY HSQC spectra of unbound (*black*) and DNA-bound (*red*) states of Myb-R2R3 labeled by [$^{12}C_{\gamma}$,$^{12}C_{\varepsilon 2}$] SAIL-Trp (0.5 mM). These two spectra were measured on a DRX800 spectrometer at 37°C. **b** The values of the chemical shift changes of the ^{1}H (*blue*) and ^{13}C (*red*) peaks in [$^{12}C_{\gamma}$,$^{12}C_{\varepsilon 2}$] SAIL-Trp upon binding to the target DNA. The *asterisk* indicates an unassigned signal. **c** The locations of the six Trp residues in the Myb-R2R3/DNA complex (PDB# 1MSE)

This NOE-based assignment scheme should, in principle, work for larger proteins. In addition, the opportunity to obtain information on the χ_2 angles is favorable for NMR structure determination, as the orientation of the indole ring, occupying a large space, affects the spatial arrangement of the surrounding atoms. Along with the SAIL-Phe and Tyr (Takeda et al. 2010), the availability of [$^{12}C_{\gamma}$,$^{12}C_{\varepsilon 2}$] SAIL-Trp has become one of the milestones toward protein structure determination including information on aromatic resonances.

Acknowledgments We thank Prof. Yoshifumi Nishimura and Dr. Aritaka Nagadoi, of Yokohama City University, for providing the Myb-R2R3 gene, and Dr. Frank Löhr, Institute of Biophysical Chemistry and Center of Biological Magnetic Resonance, Goethe-University, for his kind help in providing the NMR sequence of the ^{1}H–^{13}C TROSY experiments. This work was supported in part by the Targeted Protein Research Program (MEXT) to M.K., a Grant-in-Aid for Young Scientists (B) (23770109) to M.T. and a Grant-in-Aid for Young Scientists (B) (23770111) to Y.M.

References

Amir-Heidari B, Thirlway J, Micklefield J (2007) Stereochemical course of tryptophan dehydrogenation during biosynthesis of the calcium-dependent lipopeptide antibiotics. Org Lett 9:1513–1516

Bak B, Dambmann C, Nicolaisen F (1967) Hydrogen-deuterium exchange in tryptophan. Acta Chem Scand 21:1674–1675

Bax A, Summers MF (1986) Proton and carbon-13 assignments from sensitivity-enhanced detection of heteronuclear multiple-bond connectivity by 2D multiple quantum NMR. J Am Chem Soc 108:2093–2094

Bax A, Clore GM, Gronenborn AM (1990) Proton-proton correlation via isotropic mixing of carbon-13 magnetization, a new three-dimensional approach for assigning proton and carbon-13 spectra of carbon-13-enriched proteins. J Magn Reson 88:425–431

Billeter M, Braun W, Wüthrich K (1982) Sequential resonance assignments in protein ^{1}H nuclear magnetic resonance spectra computation of sterically allowed proton–proton distances and statistical analysis of proton–proton distances in single crystal protein conformations. J Mol Biol 155:321–346

Bodenhausen G, Ruben DJ (1980) Natural abundance nitrogen-15 NMR by enhanced heteronuclear spectroscopy. Chem Phys Lett 69:185–189

Boroda E, Rakowska S, Kański R, Kańska M (2003) Enzymatic synthesis of L-tryptophan and 5′-hydroxy-L-tryptophan labeled with deuterium and tritium at the α-carbon position. J Label Compd Radiopharm 46:691–698

Carlomagno T, Maurer M, Sattler M, Schwendiger MG, Glaser SJ, Griesinger C (1996) PLUSH TACSY: Homonuclear planar TACSY with two-band selective shaped pulses applied to C^{α}, C' transfer and C^{β}, $C^{aromatic}$ correlations. J Biomol NMR 8:161–170

Cavanagh J, Fairbrother WJ, Palmer AG, Skelton NJ, Rance M, Skelton NJ (2006) Protein NMR spectroscopy: principles and practice, 2nd edn. Academic Press, San Diego

Dunbrack RL Jr, Cohen FE (1997) Bayesian statistical analysis of protein side-chain rotamer preferences. Protein Sci 6:1661–1681

Dunbrack RL Jr, Karplus M (1993) Backbone-dependent rotamer library for proteins: applications to side-chain prediction. J Mol Biol 230:543–574

Fesik SW, Eaton HL, Olenjniczak ET, Zuiterweg ERP, McIntosh LP, Dahlquist FW (1990) 2D and 3D NMR spectroscopy employing 13C–13C magnetization transfer by isotropic mixing. Spin system identification in large proteins. J Am Chem Soc 112:886–888

Gassman PG, Van Bergen TJ (1974) Oxindoles. New, general method of synthesis. J Am Chem Soc 96:5508–5511

Graf T (1992) Myb: a transcriptional activator linking proliferation and differentiation in hematopoietic cells. Curr Opin Genet Dev 2:249–255

Grzesiek S, Bax A (1995) Audio-Frequency NMR in a nutating frame. Application to the assignment of phenylalanine residues

in isotopically enriched proteins. J Am Chem Soc 117: 6527–6531
Heidelberger C (1949) The synthesis of DL-tryptophan-beta-C14, indole-3-acetic acid-alpha-C14, and DL-tryptophan-3–C14. J Biol Chem 179:139–142
Ilić N, Cohen JD (2004) Synthesis of [^{13}C]-isotopomers of indole and tryptophan for use in the analysis of indole-3-acetic acid biosynthesis. J Label Compd Radiopharm 47:635–646
Jacob J, Louis JM, Nesheiwat I, Torchia DA (2002) Biosynthetically directed fractional ^{13}C labeling facilitates identification of Phe and Tyr aromatic signals in proteins. J Biomol NMR 24:231–235
Kainosho M, Güntert P (2009) SAIL–stereo-array isotope labeling. Q Rev Biophys 42:247–300
Kainosho M, Torizawa T, Iwashita Y, Terauchi T, Ono AM, Güntert P (2006) Optimal isotope labelling for NMR protein structure determinations. Nature 440:52–57
Kay LE, Marion D, Bax A (1989) Practical aspects of 3D heteronuclear NMR of proteins. J Magn Reson 84:7284
Lautie MF (1979) Syntheses of specifically deuterated indoles. J Label Compd Radiopharm 22:735–744
Leete E, Wemple JN (1969) Biosynthesis of the Cinchona alkaloids. II. The incorporation of tryptophan-1-^{15}N,2-^{14}C and geraniol-3-^{14}C into quinine. J Am Chem Soc 91:2698–2702
Liu Z, Yuan Q, Wang W (2009) Biosynthesis of [1-^{15}N] L-tryptophan from ^{15}N labeled anthranilic acid by fermentation of *Candida utilis* mutant. Amino Acids 36:71–73
Löhr F, Rogov VV, Shi M, Bernhard F, Dötsch V (2005) Triple-resonance methods for complete resonance assignment of aromatic protons and directly bound heteronuclei in histidine and tryptophan residues. J Biomol NMR 32:309–328
Myrset AH, Bostad A, Jamin N, Lirsac PN, Toma F, Gabrielsen OS (1993) DNA and redox state induced conformational changes in the DNA-binding domain of the Myb oncoprotein. EMBO J 12:4625–4633
Norton RS, Bradbury JH (1976) Kinetics of hydrogen-deuterium exchange of tryptophan and tryptophan peptides in deutero-trifluoroacetic acid using proton magnetic resonance spectroscopy. Molecul Cell Biochem 12:103–111
Oba M, Ueno R, Fukuoka (nee Yoshida) M, Kainosho M, Nishiyama K (1995) Synthesis of L-threo-[1-^{13}C,2,3-^{2}H$_2$] and L-erythro-[1-13C,2,3-^{2}H$_2$]amino-acids: novel probes for conformational analysis of peptide side-chains. J Chem Soc Perkin Trans 1: 1603–1609
Oba Y, Kato S, Ojika M, Inouye S (2002) Biosynthesis of luciferin in the sea firefly, *Cypridina hilgendorfii*: L-tryptophan is a component in Cypridina luciferin. Tetrahedron Lett 43:2389–2392
Ogata K, Morikawa S, Nakamura H, Sekikawa A, Inoue T, Kanai H, Sarai A, Ishii S, Yoshifumi N (1994) Solution structure of a specific DNA complex of the Myb DNA-binding domain with cooperative recognition helices. Cell 79:639–648
Osborne A, Teng Q, Miles EW, Phillips RS (2003) Detection of open and closed conformations of tryptophan synthase by ^{15}N-heteronuclear single-quantum coherence nuclear magnetic resonance of bound 1-^{15}N-L-tryptophan. J Biol Chem 278:44083–44090
Pervushin K, Riek R, Wider G, Wüthrich K (1997) Attenuated T2 relaxation by mutual cancellation of dipole–dipole coupling and chemical shift anisotropy indicates an avenue to NMR structures of very large biological macromolecules in solution. Proc Natl Acad Sci USA 94:12366–12371
Pervushin K, Riek R, Wider G, Wüthrich K (1998) Transverse relaxation-optimized spectroscopy (TROSY) for NMR studies of aromatic spin systems in ^{13}C-labeled proteins. J Am Chem Soc 120:6394–6400
Ponder JW, Richards FM (1987) Tertiary templates for proteins. Use of packing criteria in the enumeration of allowed sequences for different structural classes. J Mol Biol 193:775–791
Press WH, Flannery BP, Teukolsky SA, Vetterling WT (1986) Numerical recipes. Cambridge University Press, Cambridge
Prompers JJ, Groenewegen A, van Schaik RC, Pepermans HA, Hilbers C (1997) ^{1}H, ^{13}C, and ^{15}N resonance assignments of Fusarium solani pisi cutinase and preliminary features of the structure in solution. Protein Sci 6:2375–2384
Rajesh S, Nietlispach D, Nakayama H, Takio K, Laue ED, Shibata T, Ito Y (2003) A novel method for the biosynthesis of deuterated proteins with selective protonation at the aromatic rings of Phe, Tyr and Trp. J Biomol NMR 27:81–86
Saito I, Sugiyama H, Yamamoto A, Muramatsu S, Matsuda T (1984) Fluorescence of cis-1-amino-2-(3-indolyl)cyclohexane-1-carboxylic acid: a single tryptophan chi(1) rotamer model. J Am Chem Soc 106:4286–4287
Schrauber H, Eisenhaber F, Argos P (1993) Rotamers: to be or not to be? An analysis of amino acid side-chain conformations in globular proteins. J Mol Biol 230:592–612
Soledade M, Pedras C, Okinyo DPO (2006) Syntheses of perdeuterated indoles and derivatives as probes for the biosyntheses of crucifer phytoalexins. J Label Compd Radiopharm 49:33–45
Sørensen MD, Meissner A, Sørensen OW (1997) Spin-state-selective coherence transfer via intermediate states of two-spin coherence in IS spin systems: application to E.COSY-type measurement of J coupling constants. J Biomol NMR 10:181–186
Takeda M, Chang CK, Ikeya T, Güntert P, Chang YH, Hsu YL, Huang TH, Kainosho M (2008) Solution structure of the C-terminal dimerization domain of SARS coronavirus nucleocapsid protein solved by the SAIL-NMR method. J Mol Biol 380:608–622
Takeda M, Jee J, Ono AM, Terauchi T, Kainosho M (2009) Hydrogen exchange rate of tyrosine hydroxyl groups in proteins as studied by the deuterium isotope effect on C(zeta) chemical shifts. J Am Chem Soc 131:18556–18562
Takeda M, Ono AM, Terauchi T, Kainosho M (2010) Application of SAIL phenylalanine and tyrosine with alternative isotope-labeling patterns for protein structure determination. J Biomol NMR 46:45–49
Tanikawa J, Yasukawa T, Enari M, Ogata K, Nishimura Y, Ishii S, Sarai A (1993) Recognition of specific DNA sequences by the c-myb protooncogene product: role of three repeat units in the DNA-binding domain. Proc Natl Acad Sci USA 90:9320–9324
Teilum K, Brath U, Lundström P, Akke M (2006) Biosynthetic ^{13}C labeling of aromatic side chains in proteins for NMR relaxation measurements. J Am Chem Soc 128:2506–2507
Terauchi T, Kobayashi K, Okuma K, Oba M, Nishiyama N, Kainosho M (2008) Stereoselective synthesis of triply isotope-labeled Ser, Cys, and Ala: amino acids for stereoarray isotope labeling technology. Org Lett 10:2785–2787
Terauchi T, Kamikawai T, Vinogradov MG, Starodubtseva EV, Takeda M, Kainosho M (2011) Synthesis of stereoarray isotope labeled (SAIL) lysine via the "Head-to-Tail" conversion of SAIL glutamic acid. Org Lett 13:161–163
Tilstam U, Harre M, Heckrodt T, Weinmann H (2001) A mild and efficient dehydrogenation of indolines. Tetrahedron Lett 42:5385–5387
Torizawa T, Ono AM, Terauchi T, Kainosho M (2005) NMR assignment methods for the aromatic ring resonances of phenylalanine and tyrosine residues in proteins. J Am Chem Soc 127:12620–12626
Unkefer CJ, Lodwig SN, Silks LA, Hanners JL, Ehler DS, Gibson R (1991) Stereoselective synthesis of stable isotope-labeled L-α-amino acids: Chemomicrobiological synthesis of L-[β-^{13}C]-, L-[2′-^{13}C]-, and L-[1′-^{15}N]tryptophan. J Label Compd Radiopharm 34:1247–1256
van den Berg EMM, Baldew AU, de Goede ATJW, Raap J, Lugtenburg J (1988) Synthesis of three isotopomers of

L-tryptophan via a combination of organic synthesis and biotechnology. Recl Trav Chim Pays-Bas 107:73–81

van den Berg EMM, van Liemt WBS, Heemkerk B, Lugtenburg J (1989) Synthesis of indole and L-tryptophans specifically ^{2}H- or ^{13}C-labelled in the six-membered ring. J Recl Trav Chim Pays-Bas 108:304–313

van den Berg EMM, Jansen FJHM, de Goede ATJW, Baldew AU, Lugtenburg J (1990) Chemo-enzymatic synthesis and characterization of L-tryptophans selectively ^{13}C-enriched or hydroxylated in the six-membered ring using transformed *Escherichia coli* cells. Recl Trav Chim Pays-Bas 109:287–297

Vederas JC, Schleicher E, Tsai MD, Floss HG (1978) Stereochemistry and mechanism of reactions catalyzed by tryptophanase from *Escherichia coli*. J Biol Chem 253:5350–5354

Wang H, Janowick DA, Schkeryantz JM, Liu X, Fesik SW (1999) A method for assigning phenylalanines in proteins. J Am Chem Soc 121:1611–1612

Wüthrich K (1986) NMR of proteins and nucleic acids. Wiley, New York

Yamazaki T, Forman-Kay JD, Kay LE (1993) Two-dimensional NMR experiments for correlating $^{13}C\beta$ and $^{1}H\delta/\varepsilon$ chemical shifts of aromatic residues in ^{13}C-labeled proteins via scalar couplings. J Am Chem Soc 115:11054–11055

Yaw WM, Gawrisch K (1999) Deuteration of indole and N-methylindole by Raney nickel catalysis. J Label Compd Radiopharm 42:709–713

Yuan SS, Ajami AM (1982) Synthesis of ^{13}C and ^{15}N labelled (S)-Tryptophan. Tetrahedron 38:2051–2053